

Visual inspection of fire-damaged concrete based on terrestrial laser scanner data

Wallace Mukupa¹ · Craig Hancock¹ · Gethin Roberts² · Khalil Al-Manasir³ · Huib de Ligt¹ · Zhicong Chen¹

Received: 25 August 2016 / Accepted: 5 April 2017 / Published online: 25 April 2017
© Società Italiana di Fotogrammetria e Topografia (SIFET) 2017

Abstract Visual condition survey and inspection is typically the initial method employed in the assessment of concrete damaged by fire, and it is among the most significant non-destructive testing methods. In spite of visual inspection being simple in principle, it is capable of providing cardinal information about the condition of the fire-damaged structure and act as a basis upon which subsequent and detailed assessment methods can be founded. When concrete is exposed to various elevated temperatures, it undergoes change in its physical characteristics among others, and indicators such as change in surface texture, cracks, spalling and colour change become evident. These indicators of fire-damaged concrete can be assessed using visual inspection methods and further assessed with more advanced methods in a case where detailed investigations are needed. In this study, visual inspection of terrestrial laser scanner data of fire-damaged concrete was investigated by modelling and analysing laser intensity. An analysis of the generated intensity images from laser intensity data has proved useful and valuable in the visual inspection of concrete before and after heating. Furthermore, laser scanner geometric

data has been used in the assessment of concrete surface roughness before and after heating.

Keywords Terrestrial laser scanning · Fire-damaged concrete · Visual inspection · Assessment

Introduction

Fire is well known to be one of the factors that have severe effects on the integrity of various materials and structures as a whole and capable of causing catastrophic damage. In the event of a fire, there is need to assess the fire-damaged structure so as to guarantee safety and devise proper repair strategies. Building fires are so prevalent across the globe, and past research work has shown trends in investigating the effect and behaviour of different materials when subjected to thermal loading. Concrete as a widely used material in the construction industry has been investigated by several researchers, and according to Ingham (2009), examples of concrete structures that are susceptible to fire damage consist of buildings, tunnels and bridges.

A thorough assessment of a fire-damaged structure is normally carried out so as to ascertain the level of fire damage and to devise proper repair strategies that are cost-effective. In particular, Gosain et al. (2008) state that the assessment process should quantify the magnitude and degree of damage to structural elements, since this will determine the repair costs. Methods for inspection of fire-damaged concrete structures range from visual condition survey and inspection to more advanced techniques. Visual inspection is one of the most useful and versatile

✉ Wallace Mukupa
wallace.mukupa@nottingham.edu.cn; wallacemukupa@yahoo.com

¹ Department of Civil Engineering, The University of Nottingham Ningbo China, 199 Taikang East Road, Ningbo 315100, China

² Nottingham Geospatial Institute, The University of Nottingham, Nottingham NG7 2TU, UK

³ Faculty of Engineering, Middle East University, Amman, Jordan

non-destructive techniques (NDT), and it is normally undertaken at the initial phase when assessing concrete damaged by fire (Georgali and Tsakiridis 2005). Visual inspection can provide significant quantitative and qualitative data regarding the various degrees of thermal exposure. This rich information that can be useful in change detection and even in roughly estimating the temperature attained in fire-damaged concrete. It is of particular importance that the assessor of the fire-damaged structure has the ability to distinguish between the different indicators of distress that a structure may have encountered. These for instance include cracks, colour change, spalling and disintegration. Actually, the observation of physical characteristics of thermally damaged concrete such as surface texture and colour change has widely proved to be so useful in roughly assessing the levels of fire damage (Chew 1993). Knowledge about the physical changes of concrete when heated is also important in interpreting the findings from visual inspection, and there exists a wealth of literature on the modifications of thermally damaged concrete as reported by several researchers (e.g., Ergün et al. 2013; Ingham 2009; Annerel and Taerwe 2011). An obvious limitation of visual inspection is that it can only be conducted on external visible surfaces of the fire-damaged structure, and this implies that internal parts are not considered and so no information is obtained. This being the case, visual inspection is normally followed by employing more advanced assessment methods (Short et al. 2001) involving testing and detailed investigations.

As mentioned above, fire-damaged structures produce visible indications in relation to the level of thermal exposure, and such indications are usually traced and assessed with the use of standard visual inspection techniques and then followed by more rigorous assessment techniques if needed (Short et al. 2001). There are several on-site and off-site conventional techniques for assessing fire-damaged concrete. Some on-site methods include hammer soundings, visual inspections of colour change and physical features, whereas off-site methods involve invasive tests such as core drilling, compressive strength tests and petrographic examinations (Ingham 2009; Short et al. 2001). However, all these methods have their merits and drawbacks as mentioned in Felicetti (2013). This being the case, a summarised review of existing standard visual inspection techniques and related NDT methods for assessing fire-damaged concrete is provided as explained below.

Colombo and Felicetti (2007) described an approach to visual inspection of fire-damaged concrete using a low-cost digital camera. It is stated that digital pictures are not very accurate from the colourimetric point of view, but

they still allow slight colour variations to be recognised among different points on the same sample, and also the huge amount of data available in a single digital image allows drawing statistical trends ascribable to the inherent heterogeneity of the material. Luo and Lin (2007) also used digital images in the study of fire-damaged concrete, and in order to analyse the concrete colour changes at a preset-firing temperature, images were captured by a digital camera, and prior to photographing, the surfaces of the concrete specimens were polished off lightly about a thickness of 0.18 mm with fine sand paper in order to have better exterior for photographing. In order to capture the true colour of the concrete, white balance was adjusted prior to capturing images and a software package was developed for image analysis.

Annerel and Taerwe (2011) state that a digital camera has advantages for in field exploration and can be used for instance to study the surface colour changes of a column exposed to fire or the colour changes of concrete powder from a drilled hole. However, the use of cameras that are not always calibrated as for example in Felicetti (2004) implies that the information drawn from the pictures is based on mutual colour differences and less usable as an absolute reference. However, characterising a camera is harder than characterising a flatbed scanner, because there is no constraint on the input spectra viewed by the camera and because the lighting is less controlled. Hager (2013) investigated the use of images captured with a flatbed scanner for the purpose of assessing fire-damaged concrete. Concrete specimens were heated in an electric furnace, and after the specimens had cooled down, digital images were taken from the sample surfaces with a flatbed scanner. Annerel and Taerwe (2011) used a calibrated flatbed scanner and a spectrophotometer as techniques to measure the colour of concrete samples after fire exposure so as to trace the temperature history of the concrete, from which the corresponding fire damage could be assessed. It is stated that a spectrophotometer allows to measure colours in a fast and device independent way, resulting in absolute colours usable as a reference in both laboratory and field explorations. A flatbed scanner is less portable, but can be coupled to image analysis software by which focus is possible solely on the cement matrix.

Scanning electron microscopy (SEM) is a conventional method which is used to assess fire-damaged concrete. SEM analysis using backscattered electron and X-ray imaging requires a highly polished surface for optimum imaging and X-ray microanalysis. Rough-textured surfaces diminish the image quality by reducing contrast and poor feature definition (Annerel and Taerwe 2009). According

to Short et al. (2001), optical microscopy/image analysis applied to polished or petrographic thin sections has been used extensively in investigations of concrete microstructure, and whilst this includes phenomena related to mechanisms of deterioration in general, there was limited work related to fire-damaged concrete, and so an investigation was carried out to assess the potential of colour image analysis for assessing fire-damaged concrete. The study focused on the analysis and quantification of changes in the colour of concrete which was exposed to heating. Büyükoztürk and Rhim (1997) describe the imaging of concrete structures using the radar technique. This technique allows non-contact, rapid measurements covering large areas, but electromagnetic waves undergo high attenuation in moisture, and difficulties arise in imaging below closely spaced reinforcement. Also, the radar parameters must be carefully optimised for the desired application due to the trade-off between the penetration depth and image resolution.

Terrestrial laser scanning (TLS) technology has rapidly evolved in the area of structural health monitoring and other applications. It is worth mentioning that the authors have actually written a review paper on the use of TLS for change detection and deformation monitoring of structures and Mukupa et al. (2016a) can be consulted for more information. Olsen et al. (2010) investigated the application of TLS for structural damage detection and volumetric change analysis for a test specimen before and after it was damaged. It is stated that although TLS scans are not rapid enough to capture dynamic events for structural monitoring, TLS provides an excellent mechanism for pretest and posttest modelling and analysis. The use of TLS technology for visual inspection of fire-damaged concrete complements existing assessment techniques of fire-damaged concrete that have been mentioned above. Visual inspection and assessment has a subjective component, and so some researchers have proposed alternative procedures based for example on combining optical microscopy with colour image analysis and on digital camera colourimetry (Garlock et al. 2012). Laser scanners can also be utilised from a colourimetry point of view in that most of them have either an integrated or external camera. TLS technology has some advantages such as the whole concrete element can be scanned in a relatively short time and an average intensity value over the area concerned can be determined which would represent the whole element overcoming the challenge of cores drilled in limited areas for some conventional techniques. Scanning can be carried out on-site and at a distance which improves safety, and furthermore, laser scanning is a NDT technique (Mukupa et al. 2016b). Furthermore,

with TLS, a detailed 3D digital model of the fire-damaged structure can be obtained from TLS data and can be used as reference for another kind of data, for example, photographic or infrared thermography data can be rendered on it (Teza et al. 2009). However, laser scanners must have a clean line of sight during data acquisition, since the condition of the fire-damaged structure such as smoke or soot can affect the measurements. Furthermore, there is need to avoid unfavourable weather for scanning such as haze, rain or snow.

This study focused on the use of TLS intensity for postfire assessment of concrete which is a new area of research and with limited information, since the first study was carried out by the authors in Hancock et al. (2012) and then recently in Mukupa et al. (2016b). This research carries on the investigation into the use of laser scanning to detect fire-damaged concrete under different conditions and focused on visual inspection of fire-damaged concrete via modelling and analysing the laser returned intensity. Geometric data was also used in the assessment of concrete surface roughness. Furthermore, an analysis of intensity data to assess the difference between heated and unheated concrete was conducted. The experimental procedure for the visual condition survey and inspection of fire-damaged concrete using laser scanning technique is explained in detail. The experimental results of this technique are presented to demonstrate the feasibility and validity of the method.

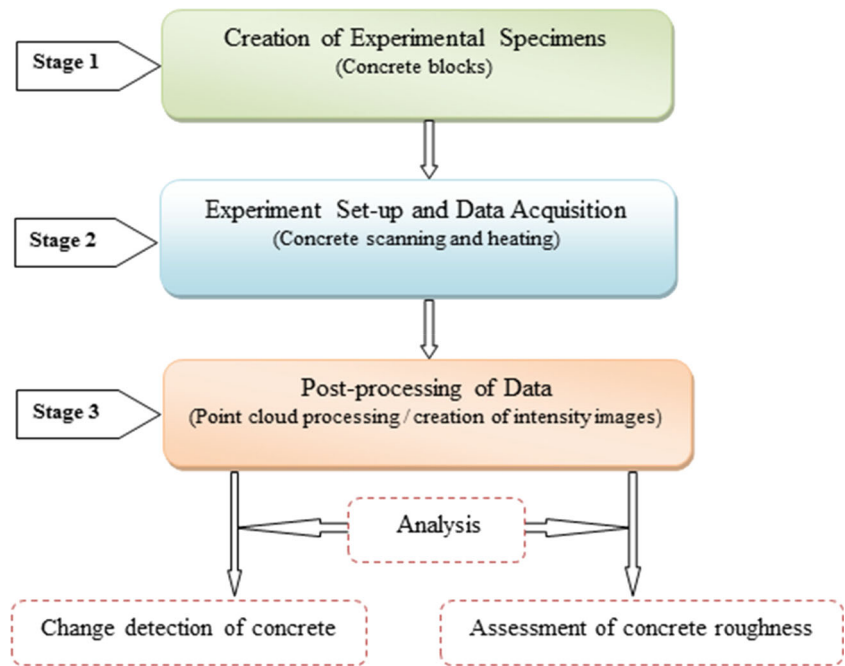
Methodology

The overall workflow of the methodology which was employed in this study is illustrated in Fig. 1 below:

With reference to Fig. 1 above, the three main stages that composed the methodology are explained as follows:

- The first stage involved creation of laboratory-sized concrete specimens and the type of concrete which was selected for this purpose is normal strength concrete (see Table 1 for details). The rationale behind the selection of this type of concrete was that it is a generic and typical mix which is meant to represent many of the concrete structures, hence adding realism to the experiments.
- The second stage consisted of setting up and conducting the experiments and these were laser scanning and heating of the concrete blocks in a furnace up to 1000 °C. Scanning of the concrete blocks was carried out in three sessions, i.e. preheating and postheating of the concrete blocks and then later after

Fig. 1 Workflow of methodology



the heated concrete blocks and the control block had been kept for a couple of months so as to assess the effects of time and environmental condition on the laser intensity. The control block was also scanned thrice, i.e. once in each scanning session. The constituents of stage two of the methodology are covered in detail from “Scanning room and equipment”, “Experiment setup for scanning”, “Data acquisition/scanning parameters” and “Thermal treatment of concrete specimens” sections. It is worth noting that the phrases ‘concrete blocks’ and ‘concrete specimens’ have been used interchangeably in this paper.

- The third stage involved postprocessing and analysing the data that was acquired. The initial steps of data processing involved filtering the scanned data so as to remove artefacts and excess data, since TLS acquires dense point data. The scans were converted to

text files (ASCII format), mainly because this format allows data to be processed and edited by many programs as the files are adapted to move freely between multiple software packages. Matlab scripts were written to process the text files which contained geometric and radiometric data of concrete. 2D intensity images were created and intensity statistics were computed for the purpose of image analysis and concrete change detection. Further analysis involved the assessment of concrete surface roughness. Detailed information about the data processing and analysis of results is presented in “Data processing” and “Results and analysis” sections.

Experiment preparation

Material and experimental specimens

Cement (composite Portland), natural siliceous river sand and siliceous coarse aggregate were used in the production of concrete specimens. Prismatic beams of dimensions $400 \times 100 \times 100$ mm were created for normal strength concrete. The concrete mix proportion and properties are given in Table 1.

The concrete specimens were taken out of the moulds after being cast for 24 h and then underwent curing in a fresh water tank for a period of 28 days. After curing, the concrete

Table 1 Material and properties of concrete specimens

Material	Water, sand, aggregate and composite Portland cement
Mix proportions	0.44:1:1.42:3.17 (Water/cement/sand/aggregate)
Water–cement ratio	0.44
Specimen size (prismatic beams)	$400 \times 100 \times 100$ mm
Curing period	28 days

specimens were kept in the civil engineering laboratory and underwent drying at room temperature.

Scanning room and equipment

The experiments were carried out in a controlled laboratory. The factors that have an influence on the laser returned intensity under such conditions are the scanning geometry and the instrumental effects. Since the experiments were carried out in a controlled environment and at short range, atmospheric losses were neglected. Scanning of the concrete specimens was carried out using Leica's HDS7000 laser scanner (Fig. 2) and shown in Table 2 are the technical specifications of the scanner.

Experiment setup for scanning

The concrete blocks were placed on a steel frame at roughly the same height as the scanner to ensure normal incidence of the laser (shelf A in Fig. 3) and the scanning distance was 3 m. The whole essence of optimising the measurement setup was based on the fact that in theory, an increase in scanning incidence angle and distance leads to a decrease of the backscattered laser intensity (Kaasalainen et al. 2011). Higher angles of incidence of for instance greater than 20° lead to poor geometry of intersection and have an effect on the precision of range determination. Furthermore, Bitenc et al. (2010) state that the random range error indicated in the scanner technical specifications only holds when scanning is carried out at normal incidence to the object that is scanned. Therefore, the range error (RE) as a result of

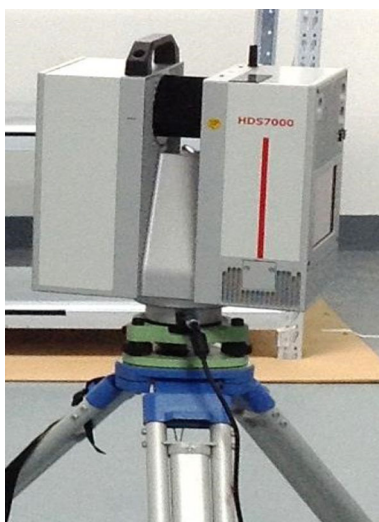


Fig. 2 HDS7000 laser scanner

Table 2 Specification of TLS instrument

Scanner	Leica HDS7000
Ranging method	Phase
Wavelength	1500 nm
Field of view (Ver/Hor)	320° × 360°
Laser class	1
Range	0.3–187 m
Linearity error	≤1 mm
Samples/s	1,016,000
Beam diameter	~3.5 mm at 0.1 m
Beam divergence	<0.3 mrad
Temp range	0–45 °C
Colour	External
Weight	9.8 kg

Source: Leica Geosystems (2012)

scanning at non-normal incidence and the effect that this has on the laser point positioning error for both the vertical and horizontal is illustrated in Fig. 3 in the case of scanning the block on shelf B.

Bitenc et al. (2010) used a pulse laser scanner and calculated the range error as shown in Eq. (1) below:

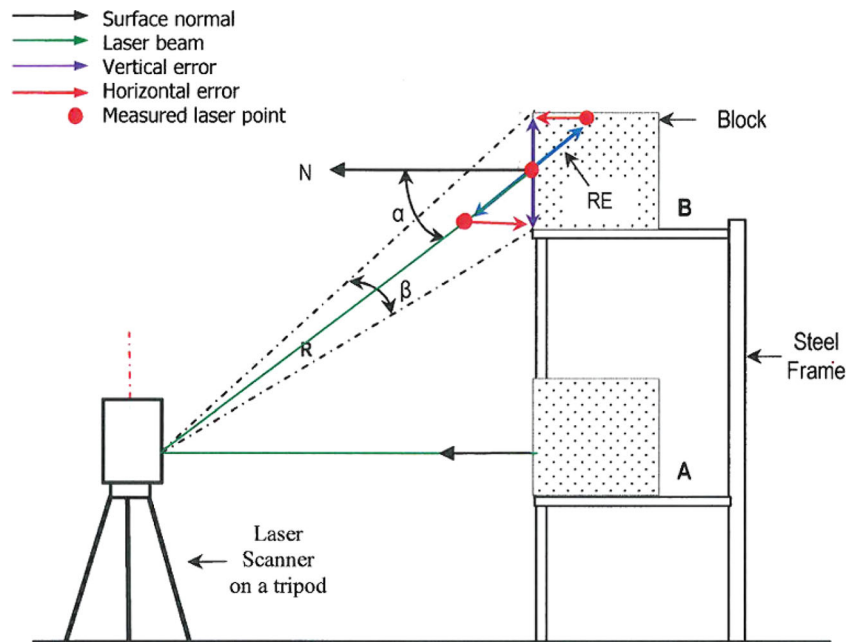
$$RE = \frac{R \cdot \beta \cdot \tan \alpha}{2}, \quad (1)$$

where RE is the range error, R is the range, β is the divergence of the laser beam and α is the angle of incidence. In this study, the scanning distance only had an error of a few millimetres because an effort was made to scan as close as possible perpendicular to the concrete specimens.

Data acquisition/scanning parameters

The scanning parameters for the HDS7000 scanner used in the experiments were set as follows: a resolution of super high and the quality as normal in order to have reasonable high redundancy and a point spacing of a few millimetres. The advantage of the scanner used is that it has touch screen operations with intuitive interfaces which were helpful during the measurement setup. Furthermore, the scanner is a survey grade instrument, and it has a digital bubble which was utilised to accurately level the instrument throughout the data acquisition sessions.

Fig. 3 Scanning the block at normal incidence and the range error at non-normal incidence. Modified from Bitenc et al. (2010).



Thermal treatment of concrete specimens

After the unheated concrete specimens were scanned with the laser scanner, they had to undergo heating, and a Carbolite CWF 12/23 electric furnace (Fig. 4) was used for this purpose. Prior to heating the concrete specimens, the furnace was tested, whereby its recorded temperature was also verified by measurements that were taken using a

dual laser infrared thermometer (Fig. 5). For easy identification, the concrete specimens were labelled as Block C, Block 1, Block 2, Block 3 and Block 4. The specimens, Blocks 1 to 4, were then heated according to the specifications shown in Table 3. The peak temperatures were maintained for 1 h to simulate fire exposure time, and after that, the furnace was switched off with the specimen inside and left to cool down to room temperature in order to avoid

Fig. 4 Carbolite CWF 12/23 electric furnace, shown is the exterior and the chamber





Fig. 5 Infrared thermometer

thermal shock. One specimen (Block C) was left unheated to act as a control/reference when comparing results with those of the other blocks that were heated.

Data processing

Scan data preprocessing

The HDS7000 scans were converted to text files using the Z + F laser control software (Zoller + Fröhlich 2013). The scans which were converted to text files contained the geometric data in terms of the X , Y and Z coordinates as well as radiometric data, i.e. the intensity values for the 3D coordinates. The intensity values of data converted to text files were ranging from -2047 to $+2048$. The Cartesian coordinates of the point cloud are computed via transforming the measured spherical coordinates to a Cartesian coordinate system as shown in Eq. (2):

$$\begin{bmatrix} x_i \\ y_i \\ z_i \end{bmatrix}_{i=1\dots n} = \begin{bmatrix} p_i \cos \phi_i \cos \theta_i \\ p_i \cos \phi_i \sin \theta_i \\ p_i \sin \phi_i \end{bmatrix}_{i=1\dots n}, \quad (2)$$

where parameters are defined as horizontal angle θ , vertical angle ϕ and the range p from the scanner to the target object,

Table 3 Specifications for concrete heating

	Block 1	Block 2	Block 3	Block 4
Temperature (°C)	250	400	700	1000
Ramping rate	10 °C/min			

considering the scanner to be the centre for the coordinate system. Reversely, the Cartesian coordinates were converted to spherical (range, zenith and azimuth angles) coordinates based on a zero origin for the TLS instrument as described in Eq. (3) (Soudarissanane et al. 2009).

$$\begin{bmatrix} p_i \\ \theta_i \\ \phi_i \end{bmatrix}_{i=1\dots n} = \begin{bmatrix} \sqrt{x_i^2 + y_i^2 + z_i^2} \\ \tan^{-1} \left(\frac{y_i}{x_i} \right) \\ \tan^{-1} \left(\frac{z_i}{\sqrt{x_i^2 + y_i^2}} \right) \end{bmatrix}_{i=1\dots n} \quad (3)$$

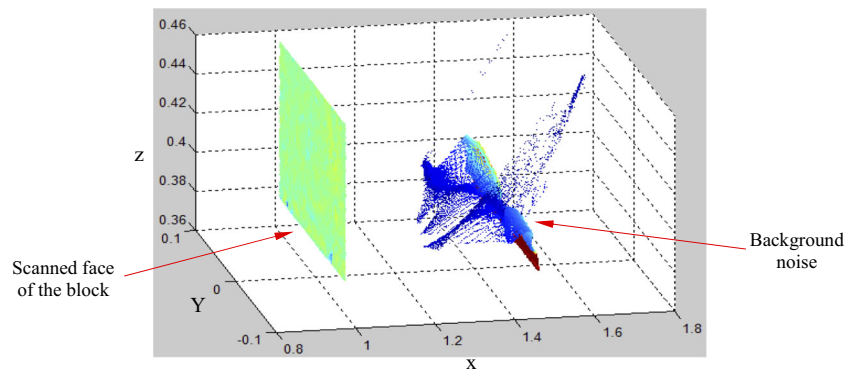
Since the laser scanner was moved in between the scanning sessions, the data captured were not in the same coordinate system. To that effect, alignment and rotation of data had to be performed using developed Matlab scripts applying the polyfit and polyval functions. The rotation matrix R (Eq. 4) as applied was to rotate all the scans counterclockwise through an angle about the origin of the coordinate system.

$$R = \begin{bmatrix} \cos \theta & -\sin \theta \\ \sin \theta & \cos \theta \end{bmatrix} \quad (4)$$

The alignment strategy implemented for the scans was a vital prerequisite for the subsequent stages in data processing. The preceding steps were helpful in devising a proper way of clipping the scanned face of each block from the point cloud, and Fig. 6 illustrates part of this process.

Shown in Fig. 6 above is a point cloud consisting of the scanned face of the block and noise in the background after the initial step of data filtering. Since the scanned face of the block was the area of interest, a reasonable section of data points around this area was selected whilst leaving out the points on the edges of the block so as to avoid the problem of mixed pixels. The noise at the background of the scanned face of the block was eliminated via limiting the point cloud based on the scanning distance function, the Y and Z dimensions of the block. The error of the scanning distance at 3 m was found to be ± 2 mm. These data processing steps and others were implemented in tailor-made Matlab functions. The sample data points that covered the selected area on the scanned face of each block were more than 15,000, and it is the intensity of these points that was used to create 2D intensity images. Sample data points for each block were also

Fig. 6 Clipping the scanned face of the block



used to calculate statistics such as incidence angle, intensity mean and standard deviation. These statistics are presented and analysed in “Comparative analysis of heated and unheated concrete” section. It is worth stating that the intensity value is dimensionless.

Generation of 2D intensity images

Intensity images were generated using intensity data for the control, unheated and the heated concrete blocks. The procedure employed was implemented in a Matlab script, and it involved creating a grid covering the Y and Z directions on the scanned face of each block and where the X direction was treated as the direction from which the image should be viewed. A grid size (g) of 0.001 m was chosen so as to produce images of good quality, and the linear interpolation technique was applied using the intensity value at each location so as to create a surface rather image covering the entire face of each concrete block. The procedure for generating 2D intensity images is illustrated in Fig. 7. Other interpolation techniques such as spline, cubic and nearest neighbour were also explored, but there were no significant differences in the images that were created using these techniques.

Determination of surface roughness

According to Carrea et al. (2016), an object can be considered to have a rough surface and behave like a diffuse target if the

root mean square height in terms of the relief that it has is greater than the expression below:

$$\lambda / 4.4 \cos \alpha, \tag{5}$$

where λ is the LiDAR wavelength and α is the incidence angle. Based on this criterion, all objects of a rocky nature can be regarded as rough surfaces relative to wavelengths spanning the range 500 to 2000 nm. The above criterion was applied to the concrete blocks that were used in this study, but it could not hold since the blocks were fairly smooth though with some minor irregularities in the magnitude of millimetres to centimetres. This being the case, the surface roughness of the blocks before and after heating was assessed by way of fitting a polynomial plane on the face of each concrete block thereafter computing the root mean square error of the fit.

Results and analysis

Visual inspection of concrete intensity images

Visual inspection is normally the initial step in the assessment of fire-damaged concrete. Table 4 shows a comparison of unheated and heated concrete intensity images. The status of Block C (the control block) remained the same, since it was unheated and acted as

Fig. 7 An illustration for generating 2D intensity images

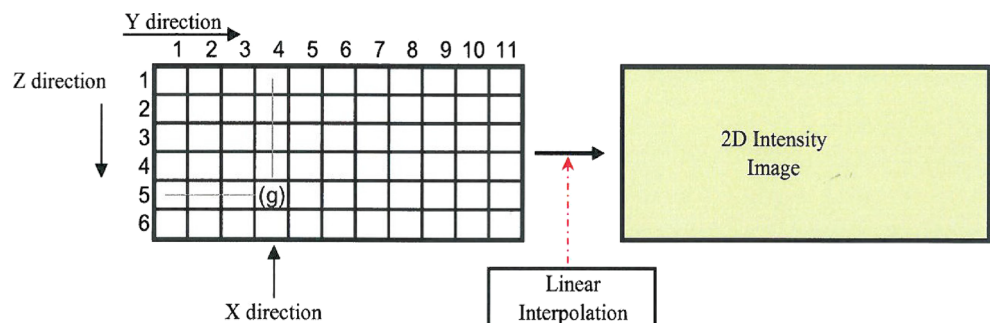
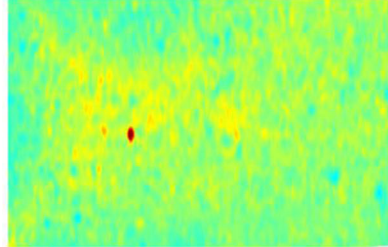
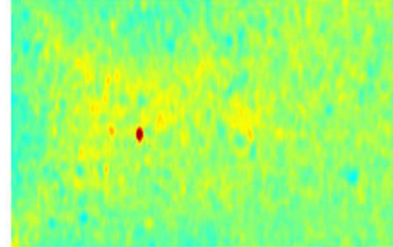
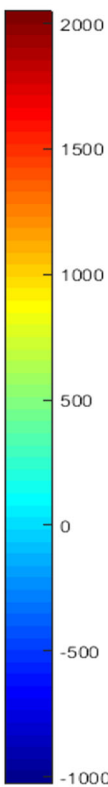
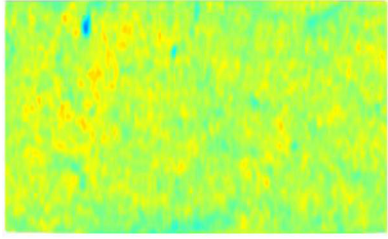
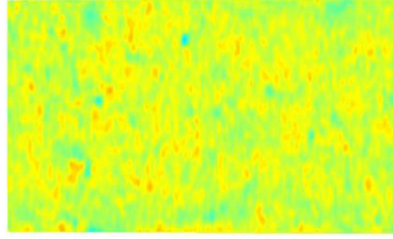
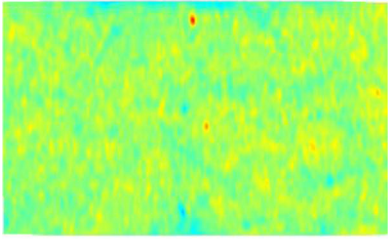
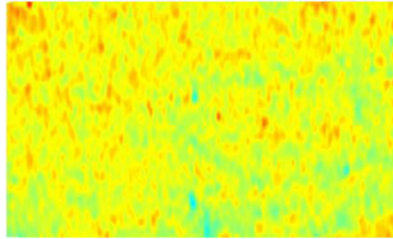
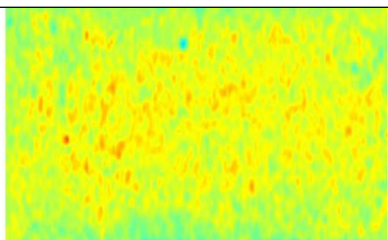
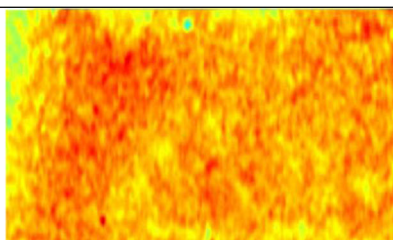
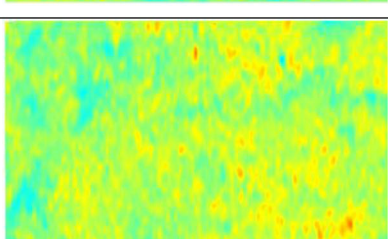
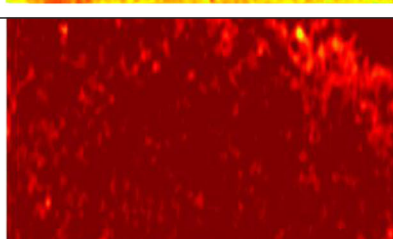


Table 4 Intensity images of control, unheated and heated concrete blocks

Block	Before and After Experiments (Same status of control block)		Intensity Range
Block C Control (Unheated)			
Block	Before Heating	After Heating	
Block 1 (250°C)			
Block 2 (400°C)			
Block 3 (700°C)			
Block 4 (1000°C)			

a reference. However, the blocks that were heated to various temperatures show remarkable differences, and it can be seen that the intensity values increase after heating which is useful in roughly assessing the change in state of heated concrete. Furthermore, visual

inspection of concrete intensity images is informative, it well complements existing visual inspection methods of fire-damaged concrete and it has the potential to act as a basis upon which to employ detailed laboratory investigations.

RGB patterns in heated concrete intensity images

RGB image analysis of heated concrete intensity images was performed using ImageJ software package (Rasband 2016). An analysis of heated concrete intensity images was carried out in an effort aimed at tracing the pattern of the RGB channels. Figures 8 and 9 below show the results of the distribution of the three primary RGB grayscale, i.e. red, green and blue for the concrete blocks

that were heated at different designated temperatures. Colour changes can be useful in identifying the extents of fire-damaged concrete (Ingham 2009), and it has been widely reported that a significant loss in strength occurs when concrete is heated above 300 °C and that normally this coincides with a concrete colour change of red or pink (Chew 1993). It can be observed from Fig. 8 for Block 1 that the area covered by the green pixels is more followed by the red and then blue is the least. A similar

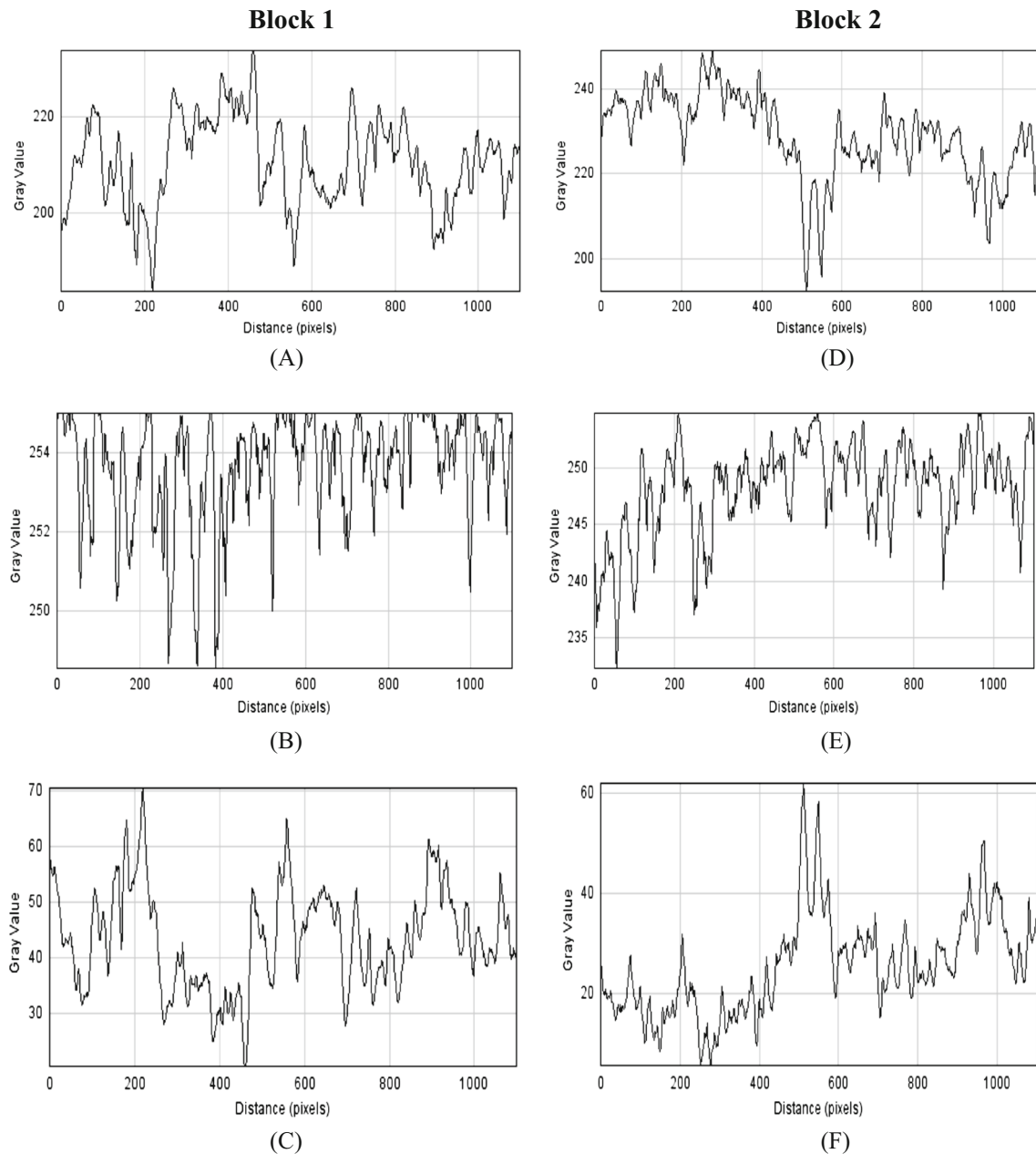


Fig. 8 Profile plots of heated concrete. The plots A, B and C are red, green and blue profile plots, respectively, for Block 1 (250 °C) and the

plots D, E and F are red, green and blue profile plots, respectively, for Block 2 (400 °C)

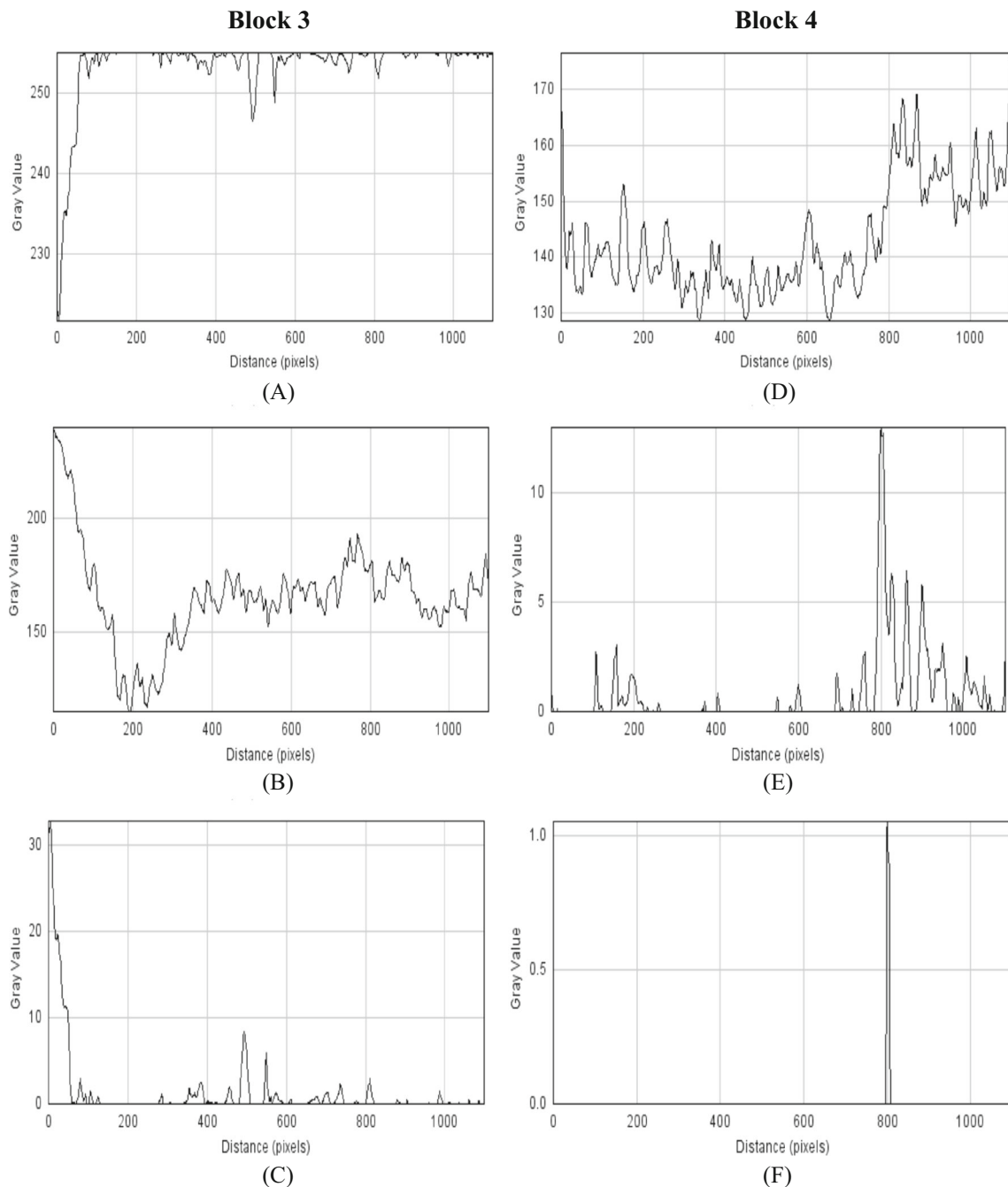


Fig. 9 Profile plots of heated concrete. The plots A, B and C are red, green and blue profile plots, respectively, for Block 3 (700 °C) and the

plots D, E and F are red, green and blue profile plots, respectively, for Block 4 (1000 °C)

pattern for the distribution of the grayscales is repeated in Block 2 with the exception that the values for the red are higher than in Block 1 (since Block 2 was heated to 400 °C) and the blue values are lower than in Block 1.

With reference to Fig. 9 below, Block 3 has higher values for the red, followed by green and then blue is the least. In

terms of Block 4, a similar pattern as in Block 3 is reproduced where red is higher, followed by green and then blue. The difference is that for Block 4, the red, green and blue have lower values in relation to the same grayscales in Block 3.

Overall, comparing both Figs. 8 and 9, it can be seen that the RGB grayscales tend to be more pronounced for

Blocks 1 and 2 than for Blocks 3 and 4. With the exception of Block 3, the trend for the Blocks 1, 2 and 4 is that red is higher, followed by green and then blue is the least. In theory, certain colour changes have been used to give an indication of the temperature that concrete has attained in a fire as mentioned in Annerel and Taerwe (2011) for instance.

Change detection of concrete intensity images

The image subtraction technique was used to obtain a change image of the state of concrete before and after heating. The intensity images were used and in this case standardised intensity images for the unheated and the heated concrete. The image subtraction technique is carried out by subtracting the pixels from one image to another. The difference rather change is computed directly using the radiometric values of the pixels. In mathematical terms, the difference image can be written as:

$$I_d(y, z) = I_2(y, z) - I_1(y, z), \quad (6)$$

where I_2 and I_1 are images after and before heating and (y, z) are the coordinates and I_d is the difference image. In the case of no change in radiance, pixels are distributed around the mean, whereas if there is change, pixels are localised at the tails of the distribution curve (Hussain et al. 2013). For change detection, the method was

applied to all the bands so as to avoid a data representation problem when using only one band (Gomez et al. 2007), and Fig. 10 below shows the results of the change images.

The image differencing technique is capable of producing a change image which is useful in change visualisation. However, such a technique does not provide a quantitative assessment. The efficiency of the detected change between heated and unheated concrete images was assessed by way of first computing the Mahalanobis distance between unheated concrete images. A small distance at the level of a few millimetres was obtained, and this signified the high reliability of the detected change. Mathematically, the Mahalanobis similarity measure between two images A and B can be written in the following form (Gomez et al. 2007):

$$S(A, B) = (\overline{A} - \overline{B})^T \Sigma^{-1} (\overline{A} - \overline{B}) \quad (7)$$

$$\Sigma = \frac{1}{N-1} \left(\sum_{i=1}^N (A_i - \overline{A})(A_i - \overline{A})^T + \sum_{i=1}^N (B_i - \overline{B})(B_i - \overline{B})^T \right), \quad (8)$$

where A_i and B_i represent the images and their respective pixel intensities, \overline{A} and \overline{B} represent average intensities for the pixels and then N being the pixels count.

Fig. 10 Change images lettered a to d are for Blocks 1 to 4, respectively, and show the change due to heating

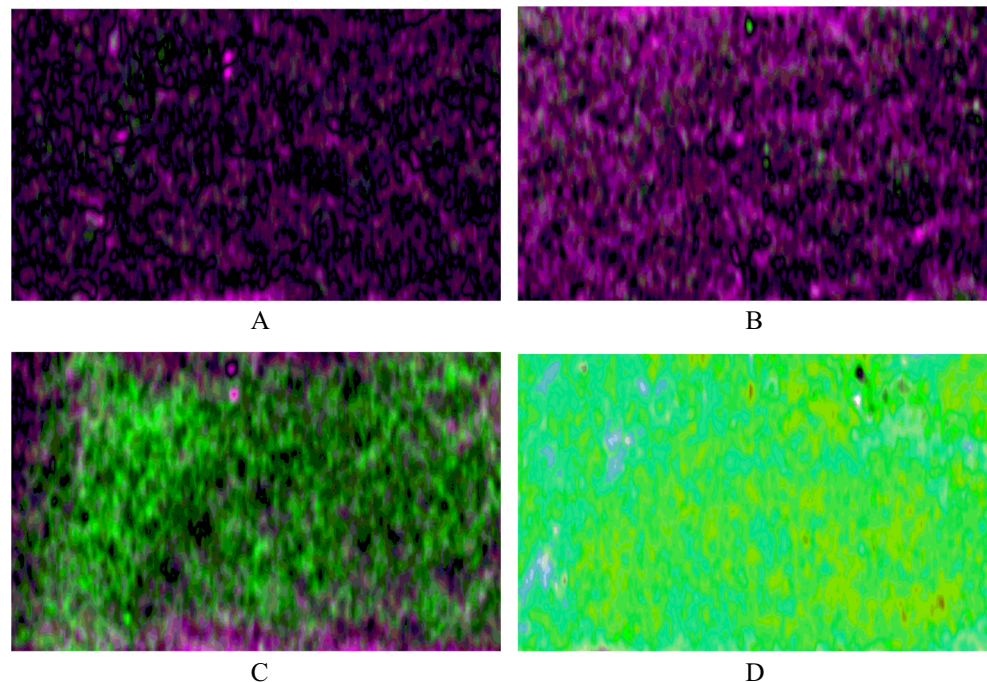


Table 5 Intensity images for the control and heated concrete blocks

Block	First Scan Intensity	Second Scan Intensity	Intensity Range
Block C Control (Unheated)			
Block 1 (250°C)			
Block 2 (400°C)			
Block 3 (700°C)			

Fig. 11 Surface roughness of unheated and heated concrete blocks

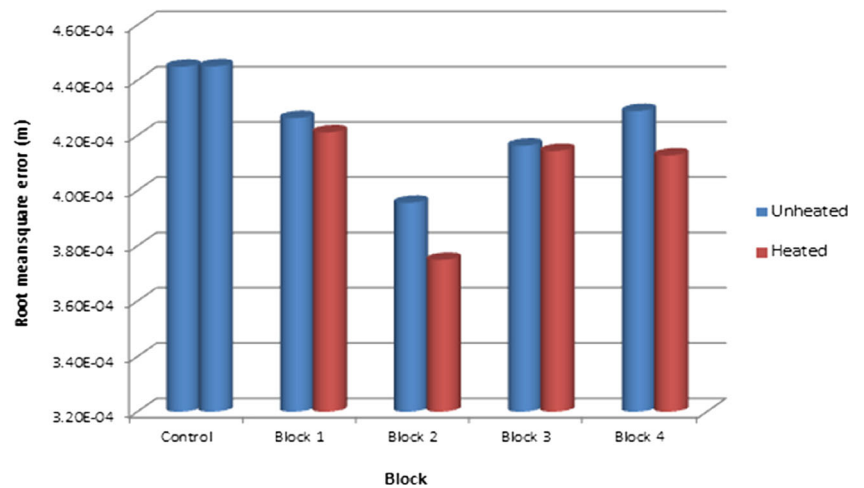


Table 6 Statistics for concrete blocks

Scanning incidence angle (°)	Scanning session	Intensity (unitless)	Block condition	Block ID				
				Block C (control)	Block 1 (250 °C)	Block 2 (400 °C)	Block 3 (700 °C)	Block 4 (1000 °C)
0.03°	1st	Mean	Unheated	559.85	660.29	573.59	755.86	627.31
			Heated	–	741.94	813.98	1129.80	1980.00
	2nd	Std. deviation	Unheated	566.12	–	–	–	–
			Heated	109.43	107.88	115.09	126.62	122.91
	1st	Std. deviation	Unheated	109.43	107.88	115.09	126.62	122.91
			Heated	–	111.69	121.50	150.81	146.07
2nd	mean	Unheated	110.96	–	–	–	–	

Concrete intensity vis-à-vis effects of time and environmental condition

An assessment of the effects of time and environmental condition on the intensity for heated concrete blocks and the control block was carried out. After scanning the heated concrete blocks for the first time in a controlled environment, these concrete blocks as well as the control block were then kept in a room with different environmental conditions such as damp for a period of 9 months, and they were then scanned for a second time. The block which was heated to a temperature of 1000 °C was not available during the second scanning session as it was fragile and disintegrated a week after the initial scanning. The result of the effect of different environmental conditions for the second scanning sessions was observed by the decrease in the intensity of the concrete blocks as shown in Table 5. Other than the different environmental conditions of a room, heated concrete tends to be hygro-

scopic and the moisture that the concrete absorbs has an influence of reducing the amount of laser returned intensity.

Assessment of concrete surface roughness

It is obvious that concrete undergoes some physical modifications when subjected to heating, and one such change is surface roughness. As a way of assessing surface roughness of concrete blocks before and after heating, the root mean square errors of the faces of the concrete blocks to the fitted plane were computed. The control block was also included in the assessment of surface roughness. Figure 11 below shows the results where change in surface roughness can be seen, although it is worth stating that the root mean square errors are relatively small, and this is attributed to the fact the concrete used in this study was fairly smooth and with minor rugosity.

Fig. 12 Comparison of unheated and heated concrete blocks based on the intensity mean

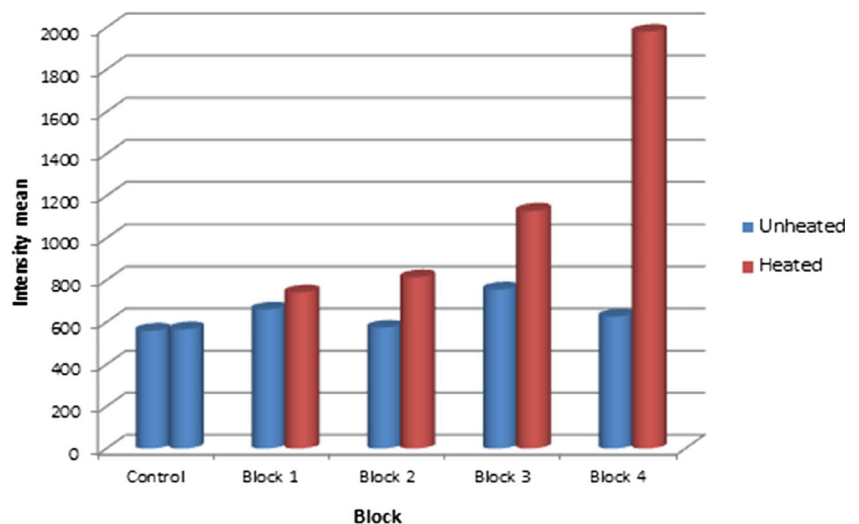
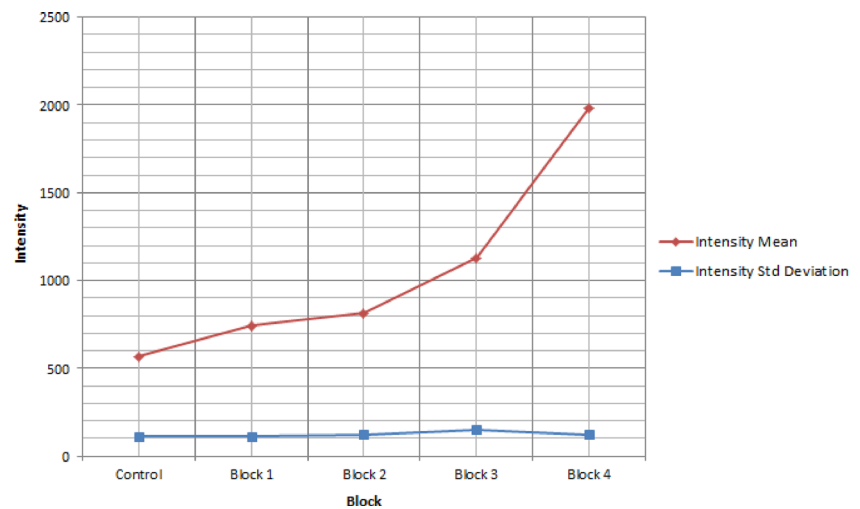


Fig. 13 Comparison of the intensity mean and intensity standard deviation for the control and heated concrete blocks



Comparative analysis of heated and unheated concrete

The computed mean intensity and mean standard deviation for the heated and unheated concrete blocks which are presented in Table 6 were used to perform the comparative analysis so as to assess the effect of thermal treatment on the returned intensity for the blocks and further relate this to the exposure temperature that each block was heated to.

The results of the comparative analysis based on the intensity mean are shown in Fig. 12, and it can be seen that for all the blocks, there is an increase in intensity after heating, and furthermore, this increase in intensity correlates well with an increase in exposure temperature for the blocks. In terms of percentage change from the initial unheated state, Blocks 1 to 4 changed by 12, 42, 49 and 216%, respectively.

A relation between the intensity mean and the intensity standard deviation is shown in Fig. 13 for the heated concrete blocks and the control block. It can be observed that the intensity mean compared to the intensity standard deviation is able to better show an increase in intensity in relation to the various temperatures that the blocks were heated to. However, the intensity standard deviation does show a minimal increase in intensity up to Block 3 and then it starts to decrease.

Conclusions and future research

A method that employs laser scanning for visual inspection and detection of fire-damaged concrete was investigated. The results that have been achieved in this study clearly demonstrate the feasibility and significance of using terrestrial laser

scanning data for visual inspection and detection of fire-damaged concrete. The method investigated is useful in quick visual inspection of a fire-damaged structure and provides more information compared to photographs captured with a digital camera. The information obtained from visual inspection is useful in determining whether to employ detailed investigation methods. The following main points can be drawn from the study:

- i. Analysis of intensity images generated from intensity data is a valuable factor in visual inspection of fire-damaged concrete and furthermore change detection can be performed based on the intensity images which is useful in change visualisation.
- ii. RGB pattern in the heated concrete intensity images showed that the red gray values are higher than the blue for the whole temperature range investigated. RGB analysis is useful in roughly assessing heated concrete.
- iii. Concrete surface roughness can be assessed using geometric data and provide an idea of surface texture and physical characteristics before and after heating.
- iv. The intensity values of concrete increased after heating and with an increase in exposure temperature implying that laser intensity can be used to detect heated and unheated concrete.

Future research will investigate the use of TLS intensity for classification of the various degrees of fire-damaged concrete for different types of concrete that will be heated to elevated temperatures. However, the current laser operates only within a very narrow spectral range, restricted to a single band, often in the near-infrared, and so the intensity values may only be practical for differentiating major material differences (Buckley et al. 2012). This being the case, laser scanners that

use different wavelengths will have to be used in the experiments, and furthermore, the use of reflectance spectroscopy across the visible near- and short-infrared spectral region will be considered for a thorough assessment of fire-damaged concrete and validation of results.

Acknowledgements The authors express their gratitude to the University of Nottingham Ningbo China for the research facilities which made this study to be undertaken. This work is partially supported by “GIS-BIM application in green built environment” innovation team under grant Ningbo Science and Technology Bureau (2015B11011) and also supported by the Ningbo Science and Technology Bureau as part of the Project “Structural Health Monitoring of Infrastructure in the Logistics Cycle” (2014A35008). Many thanks also to the FIG Foundation for the scholarship of the PhD student.

References

- Annerel E, Taerwe L (2009) Revealing the temperature history in concrete after fire exposure by microscopic analysis. *Cem Concr Res* 39(12):1239–1249
- Annerel E, Taerwe L (2011) Methods to quantify the colour development of concrete exposed to fire. *Constr Build Mater* 25(10):3989–3997
- Bitenc M, Lindenbergh R, Khoshelham K, van Waarden AP (2010) Evaluation of a laser land-based mobile mapping system for monitoring sandy coasts. *International Archives of Photogrammetry, Remote Sensing and Spatial Information Sciences* 38(Part 7B):92–97
- Buckley SJ, Kurz TH, Scheider D (2012) The benefits of terrestrial laser scanning and hyperspectral data fusion products. *International Archives of Photogrammetry, Remote Sensing and Spatial Information Sciences* 34(B7):541–546
- Büyükoztürk O, Rhim HC (1997) Radar imaging of concrete specimens for non-destructive testing. *Constr Build Mater* 11(3):195–198
- Carrea D, Abellan A, Humair F, Matasci B, Derron M, Jaboyedoff M (2016) Correction of terrestrial LiDAR intensity channel using Oren–Nayar reflectance model: an application to lithological differentiation. *ISPRS J Photogramm Remote Sens* 113:17–29
- Chew MYL (1993) The assessment of fire damaged concrete. *Build Environ* 28(1):97–102
- Colombo M, Felicetti R (2007) New NDT techniques for the assessment of fire-damaged concrete structures. *Fire Saf J* 42(6–7):461–472
- Ergün A, Gokhan K, Serhat BM, Mansour M (2013) The effect of cement dosage on mechanical properties of concrete exposed to high temperatures. *Fire Saf J* 55:160–167
- Felicetti R (2004) Digital camera colorimetry for the assessment of fire-damaged concrete. In: Gambarova PG, Felicetti R, Meda A, Riva P (eds) *Proceedings of the workshop, fire design of concrete structures, what now? What next?* Milan University of Technology, Milan, pp 211–220
- Felicetti R (2013) Assessment methods of fire damages in concrete tunnel linings. *Fire Technol* 49(2):509–529
- Garlock M, Paya-Zaforteza I, Kodur V, Gu L (2012) Fire hazard in bridges: review, assessment and repair strategies. *Eng Struct* 35:89–98
- Georgali B, Tsakiridis PE (2005) Microstructure of fire-damaged concrete. A case study. *Cem Concr Compos* 27(2):255–259
- Gomez DD, Butakoff C, Ersbøll E, Carstensen JM (2007) Automatic change detection and quantification of dermatological diseases with an application to psoriasis images. *Pattern Recogn Lett* 28(9):1012–1018
- Gosain NK, Drexler RF, Choudhuri D (2008) Evaluation and repair of fire-damaged buildings, structural forensics—investigation structures and their components (on-line). <http://www.structuremag.org/wp-content/uploads/2014/08/C-STRForensics-Fire-Gosain-Sept081.pdf>. Accessed on 12.05.2014
- Hager I (2013) Colour change in heated concrete. *Fire Technol* 50:945–958
- Hancock CM, Roberts GW, Bisby L, Cullen M, Arbuckle J (2012) Detecting fire-damaged concrete using laser scanning. FIG Working Week 2012, Rome, Italy, May 6–10
- Hussain M, Chen D, Cheng A, Wei H, Stanley D (2013) Change detection from remotely sensed images: from pixel-based to object-based approaches. *ISPRS J Photogramm Remote Sens* 80:91–106
- Ingham J (2009) Forensic engineering of fire-damaged structures. *Proceedings of Institution of Civil Engineers* 162:CE5
- Kaasalainen S, Jaakkola A, Kaasalainen M, Krooks A, Kukko A (2011) Analysis of incidence angle and distance effects on terrestrial laser scanner intensity: search for correction methods. *Remote Sens* 3(10):2207–2221
- Leica Geosystems (2012) HDS7000 User Manual. <http://hds.leica-geosystems.com> Accessed on 14th July 2014
- Luo HL, Lin DF (2007) Study the surface colour of sewage sludge mortar at high temperature. *Constr Build Mater* 21(1):90–97
- Mukupu W, Roberts GW, Hancock CM, Al-Manasir K (2016a) A review of the use of terrestrial laser scanning application for change detection and deformation monitoring of structures. *Surv Rev*:1–18
- Mukupu W, Roberts GW, Hancock CM, Al-Manasir K (2016b) A non-destructive technique for health assessment of fire-damaged concrete elements using terrestrial laser scanning. *J Civ Struct Heal Monit* 6(4):665–679
- Olsen MJ, Kuester F, Chang BJ, Hutchinson TC (2010) Terrestrial laser scanning-based structural damage assessment. *J Comput Civ Eng* 24(3):264–272
- Rasband WS (2016) ImageJ. U. S. National Institutes of Health. Bethesda, Maryland, USA. <http://imagej.nih.gov/ij/>. Accessed on 11th Apr 2016
- Short NR, Purkiss JA, Guise SE (2001) Assessment of fire damaged concrete using colour image analysis. *Constr Build Mater* 15(1):9–15
- Soudarissanane S, Lindenbergh R, Menenti M, Teunissen P (2009) Incidence angle influence on the quality of terrestrial laser scanning points. *International Archives of Photogrammetry, Remote Sensing and Spatial Information Sciences* 38(3/W8):183–188
- Teza G, Galgario A, Moro F (2009) Contactless recognition of concrete surface damage from laser scanning and curvature computation. *NDT & E International* 42(4):240–249
- Zoller + Fröhlich (2013) Z+F laser control software user manual. Zoller + Fröhlich GmbH, Wangen im Allgäu